

Fig. 1 (color online) Calculated production rate of H-like  $^{238}\text{U}^{91+}$  (Left) and Li-like  $^{238}\text{U}^{89+}$  (Right) utilizing  $^{238}\text{U}^{34+}$  projectile in target materials of Cu and Be respectively, displayed as a function of the projectile energy.

## References

- [1] X. Ma, W. Q. Wen, S. F. Zhang, et al., Nucl. Instr. Meth. B, (2017) <http://dx.doi.org/10.1016/j.nimb.2017.03.129>
- [2] Z. K. Huang, W.Q. Wen, X. Xu, et al., Nucl. Instr. Meth. B (2017). <https://doi.org/10.1016/j.nimb.2017.04.024>
- [3] C. Brandau, C. Kozhuharov, A. Müller, et al., Phys. Rev. Lett., 91(2003)073202.
- [4] D. Bernhardt, C. Brandau, Z. Harman, et al., Phys. Rev. A, 83(2011)020701(R).

## 3 - 10 State-selective Spontaneous Evolution of Rydberg Atoms into an Ultracold Plasma\*

Zaheer U. Syed<sup>1,2</sup>, Li Yufan<sup>1,2</sup>, Zhao Dongmei<sup>1</sup>, Ma Xinwen<sup>1</sup> and Yang Jie<sup>1</sup>

(<sup>1</sup>Institute of Modern Physics, Chinese Academy of Sciences, Lanzhou 730000, China;

<sup>2</sup>University Chinese Academy of Sciences, Beijing 100049, China)

We measured the state distribution of cold Rydberg atoms for various initially excited Rydberg levels and evolution times in order to investigate the collision-induced dynamics. The cold Rydberg atoms were excited into  $nP$  states ( $n = 20, 25, 30, \dots, 97$ ) below the ionization potential. Immediately after the excitation the hot electrons were detected as shown in Fig. 1(a), which are due to the slow ionization caused by the collision between hot Rydberg atoms and cold Rydberg atoms<sup>[1]</sup>. A pulsed electric field ( $\sim 300$  mV/cm) was applied after few microseconds and

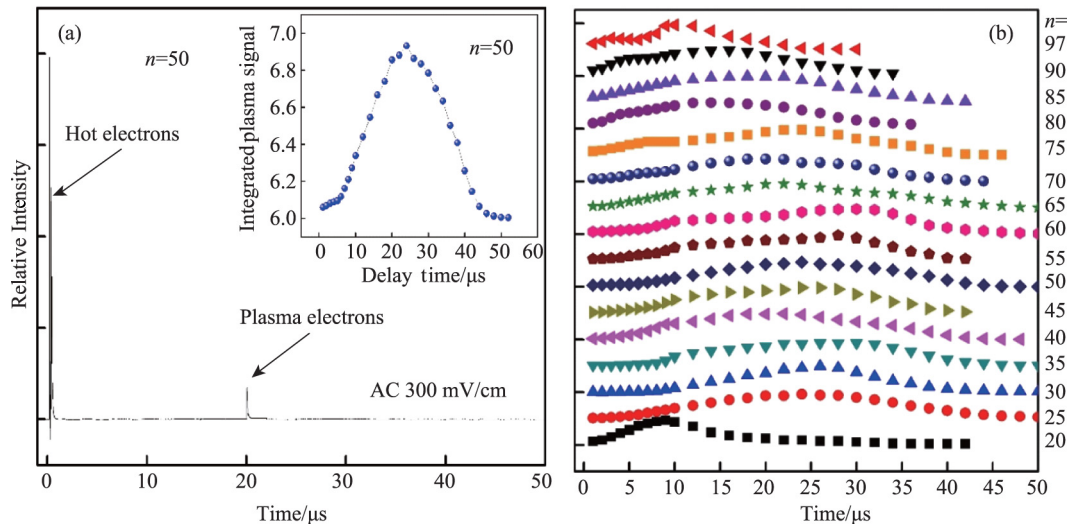


Fig. 1 (color online) (a) Electron signal for the evolution of Rydberg atoms into plasma, the inset indicates the integrated plasma signal, showing the lifetime of the plasma (b) the integrated plasma signals for different  $nP$  states.

obtained a second peak, that indicates the plasma electrons. We integrated the plasma signal for 50P state, which shows the plasma lifetime (inset Fig 1 (a)). The integrated plasma signals for all  $nP$  states are shown in the Fig 1 (b). The study of the dynamics of spontaneous ionization as a function of delay time for a broad range of initial quantum states serves to characterize the  $n$ -dependence of Rydberg–Rydberg collisional  $\ell$ -mixing, Penning ionization, and electron impact avalanche to plasma<sup>[2,3]</sup>. In Fig. 1 (b) the higher states correspond to hot collisions and blackbody radiation, the middle states indicate the dipole-dipole interaction,  $l$ -mixing, and  $n$ -mixing, while the lower states show the Penning ionization.

## References

- [1] M. P. Robinson, B. L. Tolra, M. W. Noel, et al., Phys. Rev. Lett., 85 (2000)4466.
- [2] A Walz-Flannigan, J. R. Guest, JH Choi, et al., Phys. Rev. A, 69(2004)063405.
- [3] J. Hung, H. Sadeghi, M. Schulz-Weiling, et al., J. Phys. B: At. Mol. Opt. Phys., 47(2014)155301.

\* Foundation item: National Natural Science Foundation of China (11274316, 21203216, 11404346)

## 3 - 11 Dielectronic Recombination of $^{56}\text{Fe}^{17+}$ at the CSRm\*

Khan Nadir<sup>1</sup>, Huang Zhongkui<sup>1</sup>, Wen Weiqiang<sup>1</sup>, Xu Xin<sup>2</sup>, Wang Shuxing<sup>2</sup>, Wang Hanbing<sup>1</sup>, Dou Lijun<sup>1</sup>, Zhu Xiaolong<sup>1</sup>, Mao Lijun<sup>1</sup>, Li Jie<sup>1</sup>, Ma Xiaoming<sup>1</sup>, Yang Jiancheng<sup>1</sup>, Yuan Youjin<sup>1</sup>, Zhu Linfan<sup>2</sup> and Ma Xinwen<sup>1</sup>

<sup>(1)</sup>Institute of Modern Physics, Chinese Academy of Sciences, Lanzhou 730000, China;

<sup>(2)</sup>Department of Modern Physics, University of Science and Technology of China, Hefei Anhui 230026, China)

The ionization and heating of the media surrounding accretion-powered compact sources, such as cataclysmic

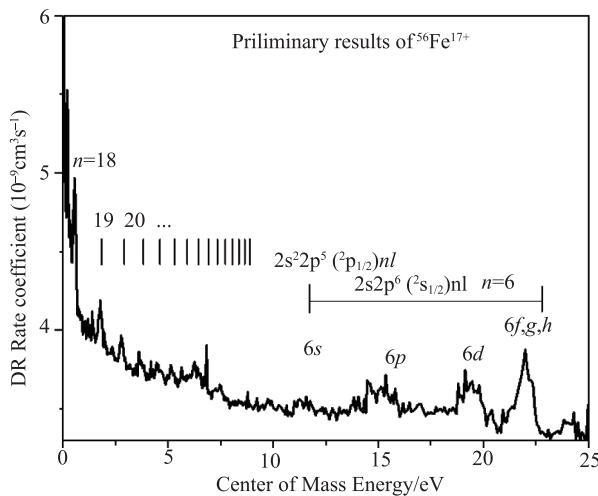


Fig. 1 (color online) The experimental DR rate coefficients for F-like  $^{56}\text{Fe}^{17+}$  ions versus the collisional energy between electron and the ion beam in the c.m. frame. The DR resonances involve  $\Delta n = 0$  transition. The observed DR channels are  $\text{Fe}^{17+}(2s^2 2p^5 [^2P_{3/2}]) + e^- \rightarrow \text{Fe}^{16+}(2s^2 2p^5 [^2P_{1/2}] nl)$  ( $n = 18, \dots$ ) and  $\text{Fe}^{17+}(2s^2 2p^5 [^2P_{3/2}]) + e^- \rightarrow \text{Fe}^{16+}(2s^2 2p^6 [^2S_{1/2}] nl)$  ( $n = 6, \dots$ ) respectively, which are indicated by vertical bars.

variables, X-ray binaries, and active galactic nuclei, are dominated by photoionization. Theoretical models of photo ionized gases show that the ionization structure is determined by photoionization balanced by radiative recombination (RR) and dielectronic recombination (DR). At low electron temperature existing in photo ionized gases with cosmic abundances, DR proceeds primarily via  $nl_j \rightarrow nl'_j$ , excitations of core electrons ( $\Delta n = 0$ ). While Iron is the most abundant heavy element in astrophysical studies<sup>[1]</sup>. So to address the needs for modeling photo ionized gases, we have initiated an experiment to measure the  $\Delta n = 0$  DR rate for iron L-shell ions. Measurement were carried out by employing electron-ion merged-beam technique at heavy ion storage ring CSRm at IMP<sup>[2]</sup>. Here we report our results for  $\Delta n = 0$  DR of  $\text{Fe}^{17+}$ , where two series of resonance peaks of  $^2P_{3/2} - ^2P_{1/2}$  and  $^2P_{3/2} - ^2S_{1/2}$  (for excitation energies 12.718 2 eV and 132.006 2 eV respectively) were observed. However because of the instability of beam line and the breakdown of electron voltage detuning system, the series limit of DR channel  $^2P_{3/2} - ^2S_{1/2}$  was not observed in these measurement as shown in Fig. 1. The further data analysis and the theoretical calculations are in progress.

## References

- [1] D. W. Savin, T. Bartsch, M. H. Chen, et al., The Astrophysical Journal, 489(1997)L115.
- [2] Z K Huang, W Q Wen, H B Wang, et al., Phys. Scr. T166(2015)014023.

\* Foundation item: National Natural Science foundation of China (11320101003) and External Cooperation Program of the CAS, (GJHZ1305)